ELSEVIER

Polymer 40 (1999) 1233–1239

polymer

# X-ray pole figures for oriented PVC

M. Gilbert[a,*], D.H. Ross[a], A. Bowen[1,b]

[a]Institute of Polymer Technology and Materials Engineering, Loughborough University, Loughborough LE11 3TU, UK
[b]DERA, Farnborough, GU14 6TD, UK

Received 22 August 1997; revised 17 March 1998; accepted 19 March 1998

## Abstract

X-ray pole figures were obtained for samples of lightly plasticised poly(vinyl chloride) which had been subjected to monoaxial (draw ratio 2) and biaxial (draw ratio 2 × 2) orientation at 70°C. These pole figures confirmed the presence of crystallite orientation and suggested the presence of two distributions of crystallites, having the *a*- and *c*-axes of the unit cell, respectively, predominantly in the stretch direction. The relative amount of *c*-axis orientation was greater in the biaxially stretched sheet, possibly at least partly owing to the presence of mesomorphous structure. © 1998 Elsevier Science Ltd. All rights reserved.

*Keywords:* X-ray pole figures; Oriented; Poly(vinyl chloride)

## 1. Introduction

The crystal structure of poly(vinyl chloride) (PVC) was first reported by Natta and Corradini[1], who showed that it possessed an orthorhombic unit cell with dimensions $a = 1.06$ nm, $b = 0.54$ nm and $c = 0.51$ nm. They also indexed the five most intense peaks observed in the X-ray diffraction pattern. The next detailed study was carried out by Wilkes *et al.*[2], who using a highly crystalline PVC sample observed a rather denser unit cell and were able to index 12 (hk0) reflections. Some additional reflections (hk1) of relatively high intensity were indexed by Guerrero *et al.*[3].

A number of publications have reported wide angle X-ray diffraction patterns for oriented PVC, as discussed in a recent review article[4]. Some early X-ray diffraction photographs of plasticised PVC demonstrated the presence of oriented crystallites[5,6]. The effect of orientation on the wide angle X-ray diffraction pattern was reported by Mammi and Nardi[7] who proposed the existence of two different types of oriented chains, namely those in oriented crystallites, and those in another phase described as mesomorphous. More recently, X-ray diffraction patterns of oriented PVC have been discussed by a number of other workers[8–14]. In 1989, Guerrero[15] demonstrated that pole figures could be obtained for both rigid and plasticised PVC samples.

It has been shown[9,10,13,14] that orientation produces increased order, resulting in increased strength in the orientation direction(s). In order to understand the nature of the crystallite orientation more fully, X-ray pole figures have been obtained for monoaxially and biaxially oriented samples of PVC.

## 2. Experimental

The PVC compound used was lightly plasticised, consisting of 100 parts by weight of suspension polymerised PVC (EVC ‘Evipol’ SH7020), 20 phr diisooctyl phthalate plasticiser (DIOP) and 2 phr Cd/Ba stabiliser (Lankromark LC68). These materials were blended using a laboratory scale Fielder High Speed mixer, then compression moulded at 180°C. Samples from the compression mouldings were then subjected to: (a) monoaxial; and (b) biaxial drawing using a straining rate of 1 mm/min, as described previously[13,14]. The samples used for this study were drawn at 70°C to a draw ratio of 2 (2 × 2 for the biaxial sample), then annealed at 70°C for 1 h.

In order to identify positions of scattering peaks, wide angle X-ray diffraction traces from 10 to 44°2$\theta$ were obtained in the reflection mode for flat rectangular samples using a Jeol DX-GE-2S generator operated at 40 kV, 30 mA with a vertical goniometer type DX-GO-S. Ni filtered Cu $K_\alpha$ radiation was used in an air atmosphere.

Preferred orientation measurements were made on an

---

[*] Corresponding author.
[1] Deceased.

*PII* S0032-3861(98)00271-7

Table 1
Calculated lattice spacings for poly(vinyl chloride)

| Miller indices (hk1) | °2$\theta$ | $d$ (nm) | $I$ (calc) (arbitrary units) |
|---|---|---|---|
| 010 | 16.42 | 0.540 | 18 |
| 200 | 16.72 | 0.530 | 41 |
| 001 | 17.39 | 0.510 | 14 |
| 110 | 18.42 | 0.481 | 100 |
| 101 | 19.29 | 0.460 | 15 |
| 210 | 23.54 | 0.378 | 40 |
| 011 | 23.99 | 0.371 | 0 |
| 201 | 24.25 | 0.367 | 71 |
| 300 | 25.23 | 0.353 | 0 |
| 111 | 25.43 | 0.350 | 74 |
| 211 | 29.37 | 0.304 | 12 |
| 310 | 30.19 | 0.296 | 17 |
| 301 | 30.83 | 0.290 | 1 |
| 020 | 33.18 | 0.270 | 3 |
| 400 | 33.83 | 0.265 | 2 |
| 120 | 34.22 | 0.262 | 2 |

automated Siemens texture goniometer operated at 40 kV and 30 mA using Cu $K_\alpha$ radiation with a graphite monochromator in the diffracted beam. Lattice spacings corresponding to possible reflections calculated for the known unit cell dimensions, and the *Pacm* space group reported for crystalline PVC[1] are shown in Table 1. Most of these spacings have been reported previously. Pole figures were measured at 16.71, 18.42, 23.50, 24.20, 25.43, 29.37, and 30.20°2$\theta$. Peaks at 16.71 and 18.42°2$\theta$ were clearly distinct from the wide angle diffraction trace. The peak centred at 24°2$\theta$ is very broad, and contributions from five different planes are expected in this region, although two would be extremely weak (Table 1). Measurements were therefore made at three different positions, corresponding to (210), (201) and (111) planes, to see if any differences could be detected. Similarly, two measurements were made in the 30°2$\theta$ region. Step sizes of 5° were used for both tilt and rotation angles, up to a maximum tilt angle of 75°2$\theta$. The raw data values were then processed by initially subtracting the background from values measured at 12 and 35°2$\theta$, then correcting for defocusing using an undrawn sample, and finally normalising to give $x$ random contours.

## 3. Results and discussion

Wide angle X-ray diffraction patterns for the two samples are shown in Figs 1 and 2. (The two sharp peaks at 33.7 and 36.4°2$\theta$ appear with varying intensity in different samples, and are believed to arise from reactions associated with the stabiliser). Both figures show enhanced scattering intensity in the 16–18°2$\theta$ region compared with undrawn compression mouldings[10]. The relative intensity of the two peaks in this region differs for the two samples. The peak at 16.7°2$\theta$ ($d = 0.531$ nm) corresponds to the (200) reflection and that at 18.42°2$\theta$ ($d = 0.481$ nm) to the (110) reflection[1–3]. The former peak is more intense in the biaxially drawn sample, suggesting that the proportion of (200) planes in the plane of this sheet is higher than in the monoaxially drawn sheet, as discussed in a recent paper[16]. The position of this peak suggests that some mesomorphous structure, with alignment parallel to the chain direction in the polymer will also be present.

Pole figures obtained for the two samples are shown in Figs 3 and 4. In these figures, the vertical stretch (machine direction) is north–south, the horizontal or transverse direction is west–east, and the sheet normal is at the centre of the pole figures. Owing to the low crystallinity of commercial PVC, and the small and varied crystallite size[4], X-ray diffraction patterns for PVC are weak and ill-defined and this is reflected in the pole figures.

In the 25°2$\theta$ region, overlapping peaks have been assigned as follows. Natta and Corridini[1] attributed a peak at 23.79°2$\theta$ ($d = 0.374$ nm) to the (210) reflection; there are also (201) ($d = 0.361$ nm) and (111) ($d = 0.344$ nm) within the same angular region[3]. Since all peaks are broad, owing to the small, imperfect crystallites

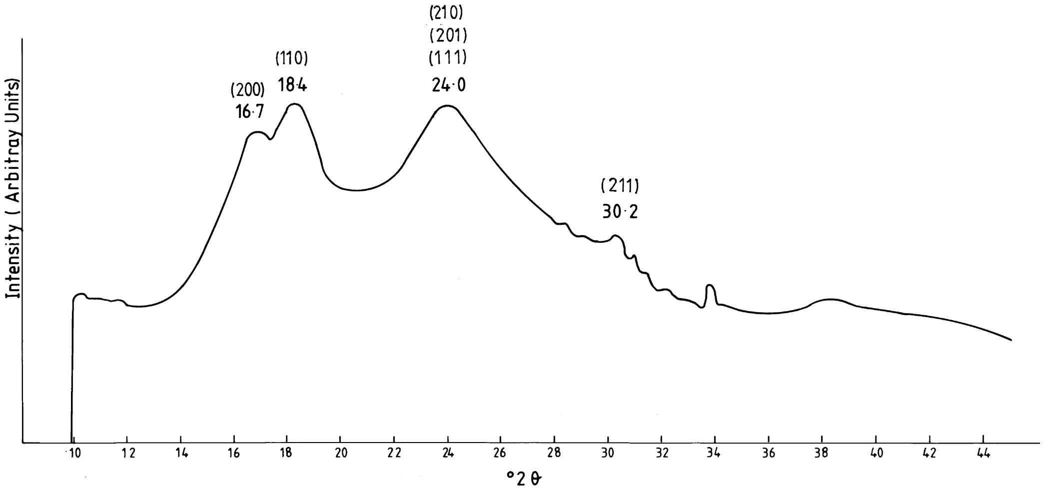

Fig. 1. Wide angle X-ray diffraction pattern for monoaxially oriented sheet.

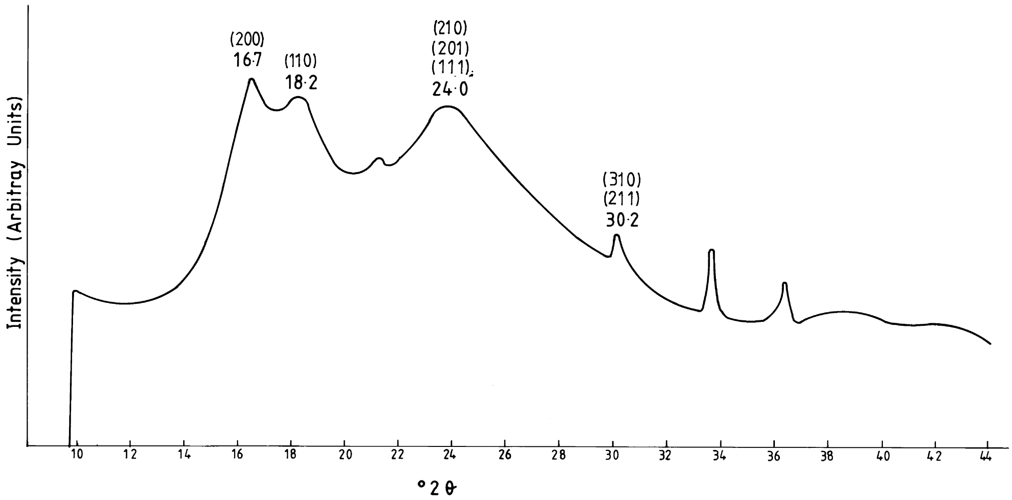

Fig. 2. Wide angle X-ray diffraction pattern for biaxially oriented sheet.

present in PVC, the peak overlap is considerable. Guerrero *et al.*[3] calculated that the relative intensity of the three peaks, $I_{(210)}$:$I_{(201)}$:$I_{(111)}$ was 34.4:72.7:66.9. In the 30°2$\theta$ angular region the observed peak has been assigned to the (310) reflection ($d = 0.294$ nm[1], 0.286 nm[2]).

### 3.1. Monoaxially oriented sheet

The (200) pole figure for this sample (Fig. 3*a*) shows that there are intensity maxima both in the sheet normal direction, with some spread in the transverse direction (i.e. perpendicular to the original draw direction), and 20–30°2$\theta$ from the stretch direction towards the transverse direction. A similar situation was observed for the 110 poles (Fig. 3*b*), except that the spread of the distribution of poles in the transverse direction was greater. Guerrero[15] presented a pole figure for a PVC sample containing 20 phr dioctyl phthalate, which also showed the highest concentration of (110) planes in the transverse direction. However, as his sample was extended to a draw ratio of 3, the concentration in the transverse direction was correspondingly greater. The similarity of the (110) and (200) pole figures was also noted in his paper.

Pole figures were obtained at 23.50, 24.20 and 25.43°2$\theta$ to correspond to (210), (201) and (111) reflections, respectively. However, because of the peak overlap mentioned above, no significant differences between the pole figures obtained at these angles could be detected. The pole figure at 25.43°2$\theta$ is shown in Fig. 3*c*, but owing to the overlap, this must include contributions from all three reflections listed above. Maximum intensities were observed in the transverse direction, at an angle approximately 50–60°2$\theta$ from the sheet normal, but spreading up to 45°2$\theta$ towards the stretch direction.

Two pole figures were also obtained in the 30°2$\theta$ region to correspond to (211) reflections (29.37°2$\theta$) and (310) reflections (30.20°2$\theta$) (Table 1). The distribution of intensities was similar in both cases, but the intensities observed were higher at 29.37°2$\theta$ (Fig. 3*d*). The distribution was rather more complex than in the other pole figures. All poles were concentrated in a region ± approximately 50° from the stretch direction towards the transverse direction. Maxima were observed from the stretch direction up to about 25° from the stretch direction, at about 40° from the sheet normal.

### 3.2. Biaxially oriented sheet

In this case, there are of course two stretch directions, resulting in planar orientation[14]. Pole figures are generally very similar to those for the monoaxially oriented sheet.

The (200) poles are again concentrated near the sheet normal, with weaker scattering 30–40° from the north–south stretch direction. From a pole figure in which different contours appear in different colours, it is apparent in the first case that maxima are actually about 10° from the sheet normal, and at 80° from the transverse direction (Fig. 4*a*). The (110) poles behave in a similar manner, except that the spread from the sheet normal is greater (Fig. 4*b*).

The three pole figures for the 24°2$\theta$ region are again similar to each other, and to those for the monoaxially oriented sample. That at 25.43°2$\theta$ is the most intense of the three, and is shown in Fig. 4*c*. The two pole figures in the 30°2$\theta$ region were again very similar to those for the monoaxially oriented sample (see Fig. 3*d* and Fig. 4*d*).

### 3.3. Crystallite orientation in oriented samples

Crystallites in PVC are believed to be thin platelets, restricted in length along the chain direction because of the limited syndiotactic order in the polymer, although a recent paper[18] proposes that certain isotactic conformations can also crystallise. Nevertheless, the broad melting range observed for PVC implies a wide range of crystallite size and perfection. Considering first the monoaxially oriented samples, the (200) pole figure suggests that there

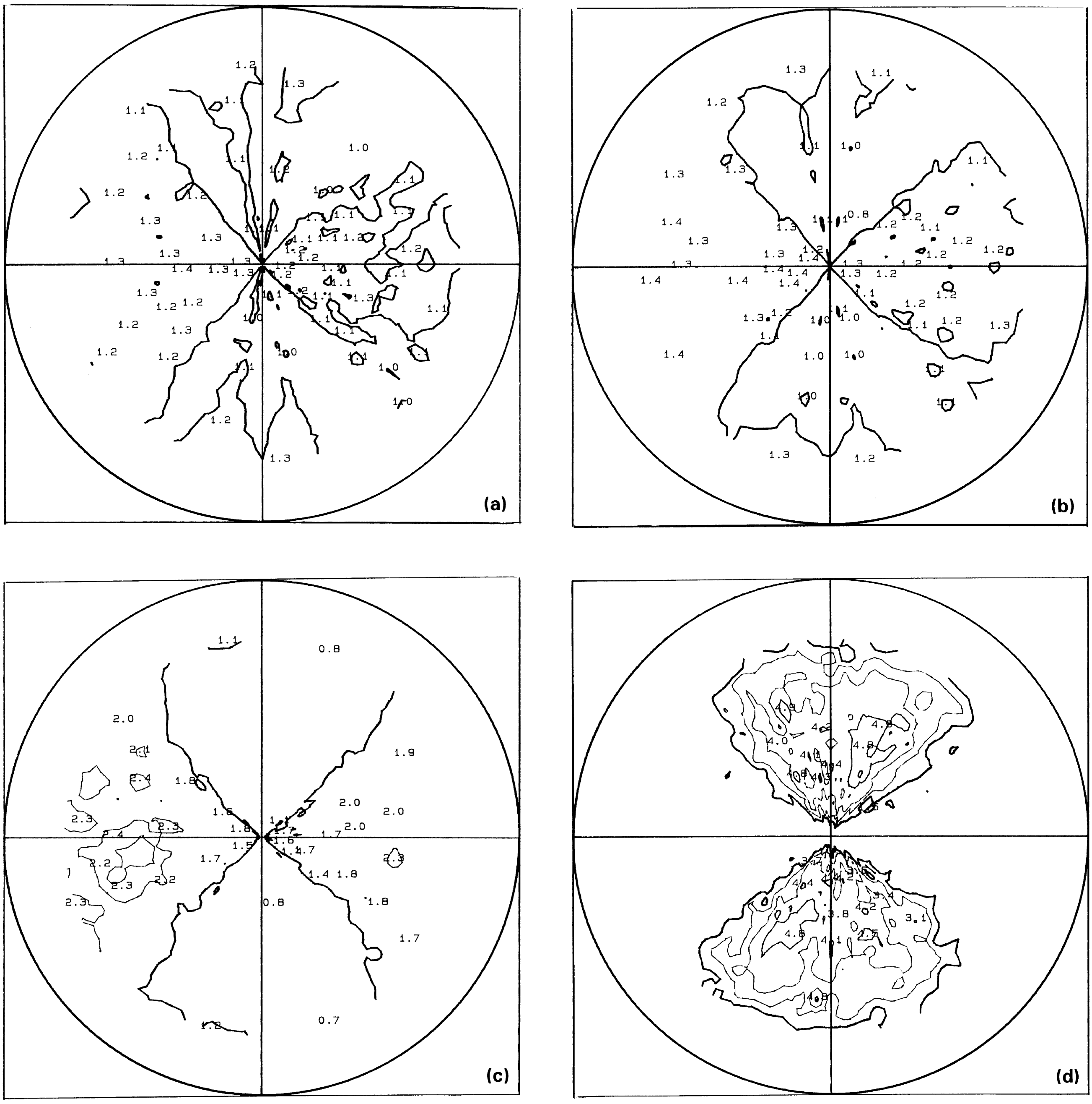

Fig. 3. Pole figures for monoaxially oriented sheet: (a) $d = 16.71°2\theta$; (b) $d = 18.42°2\theta$; (c) $d = 25.43°2\theta$; (d) $d = 29.37°2\theta$.

are two distinct unit cell orientations in the polymer. That producing a maximum at the centre implies that the *a*-axes of the unit cell are concentrated in the sheet normal direction. The similar figure for the (110) poles, with increased spread in the transverse direction, implies that the *b*-axes will be concentrated in the latter direction; hence, since the three axes are at right angles, the *c*-axes will be in the stretch direction. The remaining pole figures should be consistent with these. Examination of the unit cell for PVC shows that the (210) pole is at 45° to the (200) pole in the *ab* plane. This should produce a maximum intensity in the transverse direction, 45° towards the sheet normal, as is in fact observed in Fig. 3*c*. However, (201) and (111) reflections are also present around 25°2$\theta$. For unoriented samples, these are expected to be more intense than the (210) reflection (Table 1). The (201) pole is at 45° to the (200) pole in the *ac* plane. With the orientation described, this would be expected to produce a maximum in the stretch direction. The (111) reflection would produce maximum intensity at an angle of 27° to the stretch direction, and 45° from the sheet normal. The pole figures produced did not correspond with either of these.

The pole figure in the 30°2$\theta$ region cannot be explained by the previously reported (310) reflection, which would be

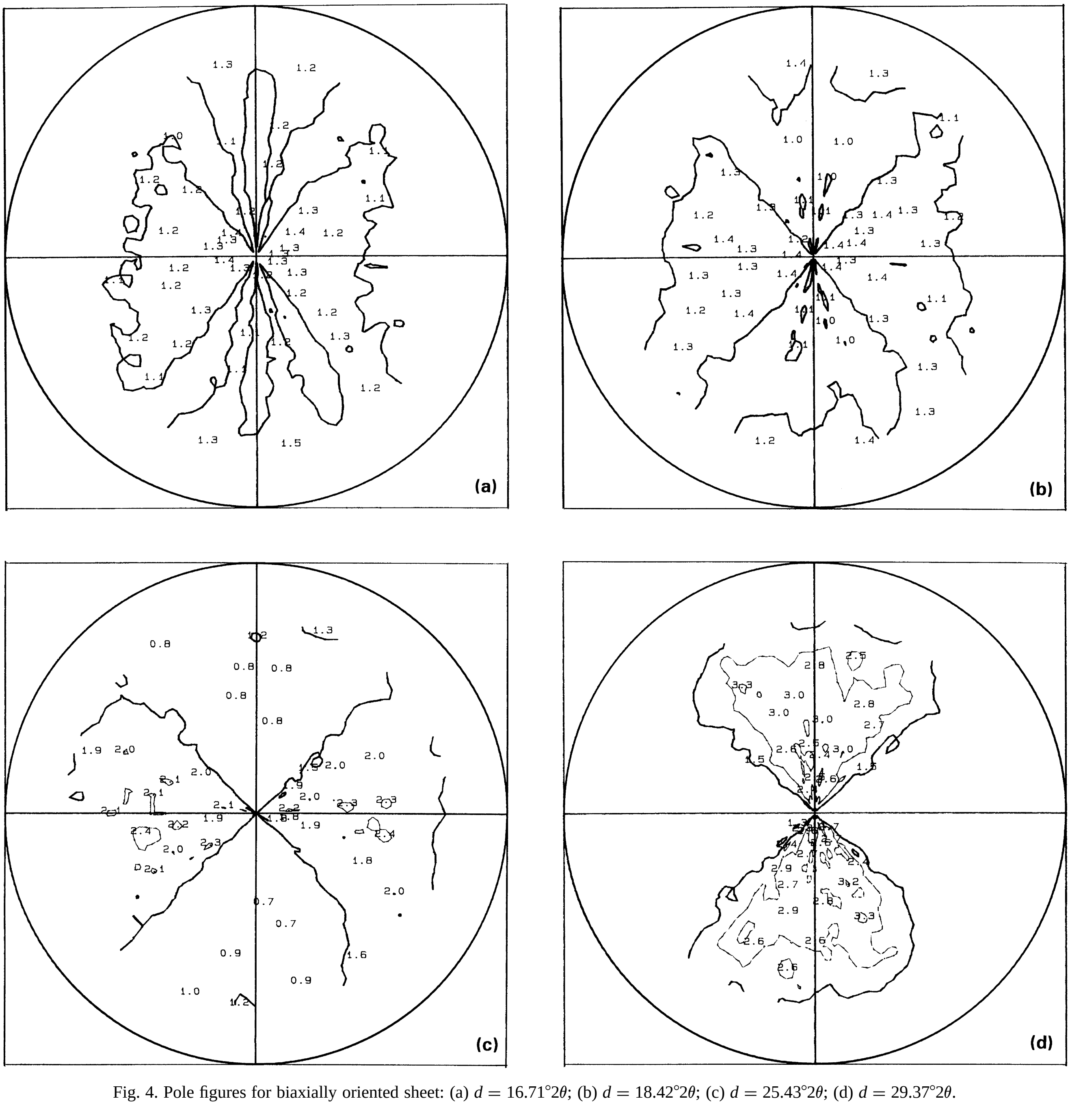

Fig. 4. Pole figures for biaxially oriented sheet: (a) $d = 16.71°2\theta$; (b) $d = 18.42°2\theta$; (c) $d = 25.43°2\theta$; (d) $d = 29.37°2\theta$.

expected to give a maximum in the transverse direction. However, calculation showed that (211) and (301) reflections may also be expected in this region at 30.20 and $30.76°2\theta$, respectively. Relative intensities of all diffractions listed in Table 1 were calculated from structure factors using the method described by Guerrero *et al.*[3], and are listed in the final column of Table 1. Although values are not identical to those obtained, diffractions listed by Guerrero are classified in approximately the same order by our results. The (211) poles would be expected to produce a maximum at 45° to the stretch direction, which is not ruled out, but would not account for the entire pattern. (301) poles would produce maxima in the stretch direction at approximately 30° towards the sheet normal, but are too weak to account for the observed pattern.

The second distribution of crystallites, giving maxima almost in the plane of the film, and 20–30° from the stretch direction, towards the transverse direction implies *a*-axis orientation in that position. Similar maxima for the (110) poles suggest that the *b*-axes are also in the film plane, so that the *c*-axes from this distribution will be lie near the sheet normal. The expected orientations of the (210) planes, within 15° of the transverse direction, and close to the plane of the film are consistent with Fig. 3*c*, while the (111) reflections could be present, but the (201) would lie close to the stretch direction and poles corresponding to this distribution would not contribute to the observed pattern. Fig. 3*d* could be attributed to the (310) and (211) poles arising from this distribution. In the first case above, *c*-axes are predominantly in the stretch direction.

Since the *c*-axis is parallel to the chain direction, this would be a likely orientation for fringed micelle type crystallites. For the second distribution, the *c*-axes lie close to the sheet normal. Both types of orientation have been reported previously. Guerrero, Keller and coworkers [12,19,20] found two crystallite distributions in gel processed, stretched PVC samples. Crystals having their *a*-axis aligned in the orientation direction were suggested to consist of lamellar platelets, produced from solution at high temperatures when the gel was cooled, while *c*-axis orientation was owing to the anticipated fringed micelle structure. Guerrero[15] later obtained pole figures which provided evidence for the two crystallite distributions described. As discussed above, the (110) patterns for drawn samples were similar in character to those shown here. (110) and (200) pole figures for pressed films

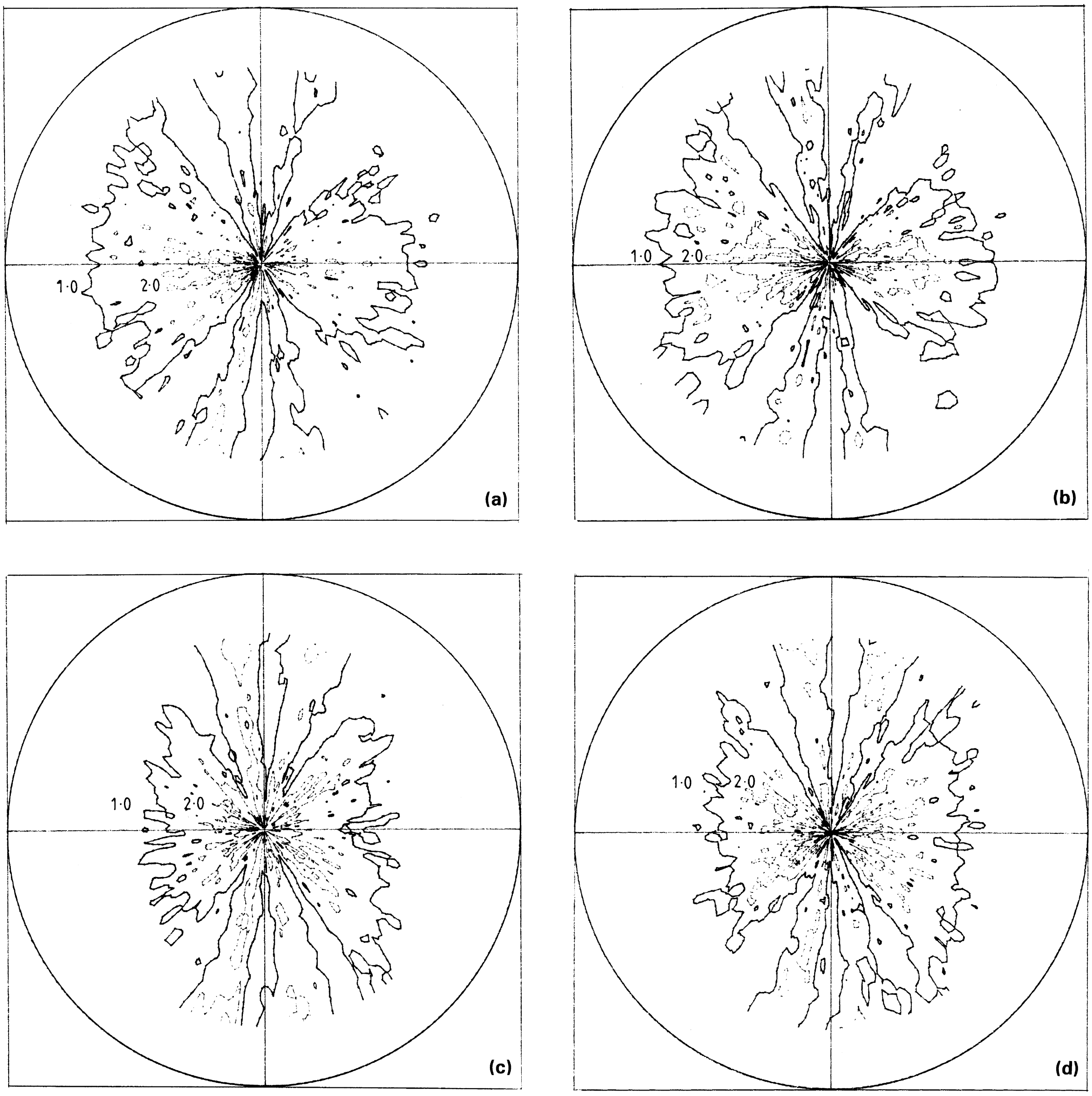

Fig. 5. Pole figures for: (a) monoaxially drawn sheet (200) planes; (b) monoaxially drawn sheet (110) planes; (c) biaxially drawn sheet (200) planes; (d) biaxially drawn sheet (110) planes.

suggested a preference for the *c*-axis to orient towards the plane of the film; those for films cast from tetrahydrofuran solution indicated a slight preference for the *c*-axis to orient perpendicular to the plane of the film. While Guerrero related *a*-axis orientation to samples produced from solution, this effect has also been reported by other workers[21,22] for samples which have not been solution cast. Robinson *et al*. used polarised Raman spectroscopy to investigate the effects of temperature and plasticiser concentration on deformation behaviour during the drawing of PVC. They made reference to the presence of some *c*-axes aligned in the draw direction, and some away from the draw direction. Tasumi and Shimanouchi postulated the existence of *a*-axis orientation from infra-red dichroism measurements on rigid PVC extended at 180°C.

At first sight, the pole figures for the monoaxially and biaxially oriented samples look surprisingly similar. Wide angle X-ray diffraction traces obtained, in the reflection mode showed that the (200) reflection was relatively stronger in the biaxially stretched sample, suggesting that the *c*-axis orientation in the plane of the film was greater in this sample, probably at least partly owing to the presence of mesomorphous structure. This has been confirmed by more detailed wide angle X-ray measurements[16], which have shown that the intensity of the (200) reflection depends not only on the type of orientation (e.g. monoaxial or biaxial), but also on the total planar orientation, obtained by multiplying draw ratios in two directions. Clearly, planar orientation is greater for the biaxially drawn sample than for the uniaxial sample. Higher *c*-axis orientation would imply higher *a*-axis orientation in the sheet normal direction. Comparison of Fig. 3*a* and Fig. 4*a* suggests that this is indeed the case, and the same trend is identified in Fig. 3*b* and Fig. 4*b*. Further differences can be observed if these four figures are reproduced with more contour lines (Fig. 5*a*–*d*). (Relative intensities for two of the sets of contour lines are indicated on these figures.) Both pole figures for biaxially oriented samples show less spread in the transverse direction, indicating that the sheet normal *a*-axis orientation in these is better defined, which is consistent with the higher planar orientation. The remaining pole figures are almost indistinguishable for the two sheets, which is unsurprising in view of their complexity as discussed earlier. Unfortunately, the pole figures obtained do not provide direct information about the orientation of the *c*-axis in the plane of the sheet, so do not correlate with property measurements on the films. Uniaxially drawn films clearly exhibit property anisotropy. Property measurements on biaxially drawn sheet[17] show that planar orientation exists, since tensile and tear properties measured in the draw directions and at 45° to these are very similar. This would imply a similar structure with regard to crystalline and amorphous orientation in all directions in the plane of the biaxially stretched sheets.

## 4. Conclusions

Despite the low level of crystallinity in PVC, and the small crystallite size, problems not encountered in the case of polyethylene which has been well studied, it has been possible to obtain pole figures from oriented samples. It has been shown that crystallite orientation does occur in these samples, as well as the orientation of chains in the amorphous region.

Pole figures for the (110) and (200) planes are consistent, and suggest the presence of two crystallite distributions. The remaining two pole figures cannot be fully explained at present. Each arises from a number of broad, overlapping reflections, and is further complicated by the presence of the two crystallite distributions.

Sheet normal *a*-axis orientation was found to be greater in the biaxially stretched sheet, owing to its higher planar orientation. This will result in a greater *c*-axis orientation in the plane of the film for this sheet.

## References

[1] Natta G, Corradini P. J Polym Sci 1965;20:251.
[2] Wilkes CE, Folt VL, Krimm S. Macromolecules 1973;6:235.
[3] Guerrero S, Meader D, Keller A. J Macromol Sci Phys 1981;B20:185.
[4] Gilbert M. J Macromol Sci Rev Macromol Chem Phys 1994;C34:77.
[5] Stein RS, Tobolsky AV. Textile Res J 1948;18:302.
[6] Alfrey T, Wiederhorn N, Stein RS, Tobolsky AV. Ind Engng Chem 1949;41:701.
[7] Mammi M, Nardi V. Nature 1963;199:247.
[8] Tsou PCK, Geil PH. Int J Polym Mater 1972;1:223.
[9] Gilbert M, Vyvoda JC. Polymer 1978;19:862.
[10] Vyvoda JC, Gilbert M, Hemsley DA. Polymer 1980;21:109.
[11] Biais R, Geny C, Mordini M, Carrega M. Br Polym J 1980;12:179.
[12] Guerrero S, Keller A, Soni PL, Geil PH. J Polym Sci Polym Phys Ed 1980;18:1533.
[13] Liu Z, Gilbert M. Polymer 1987;28:1303.
[14] Gilbert M, Liu Z. Plast Rubb Proc Appl 1988;9:67.
[15] Guerrero SJ. J Appl Polym Sci 1989;38:923.
[16] Gilbert M, Liu Z, Hitt D. J Polym Engng Sci 1997;37:1858.
[17] Hitt DJ, Gilbert M. Polym Test 1994;13:219.
[18] Hobson RJ, Windle AH. Makromol Chem Theory Simul 1993;2:257.
[19] Lemstra PJ, Keller A, Cudby M. J Polym Sci Polym Phys Ed 1978;16:1507.
[20] Guerrero S, Soni PL, Keller A, Geil PH. J Macromol Sci Phys Ed 1981;20:161.
[21] Robinson MER, Bower DI, Maddams WF. J Polym Sci Polym Phys Ed 1978;16:2115.
[22] Tasumi M, Shimanouchi T. Spectrochim Acta 1961;17:731.